Supplemental Materials

Molecular Biology of the Cell

Uehara et al.

Figure S1

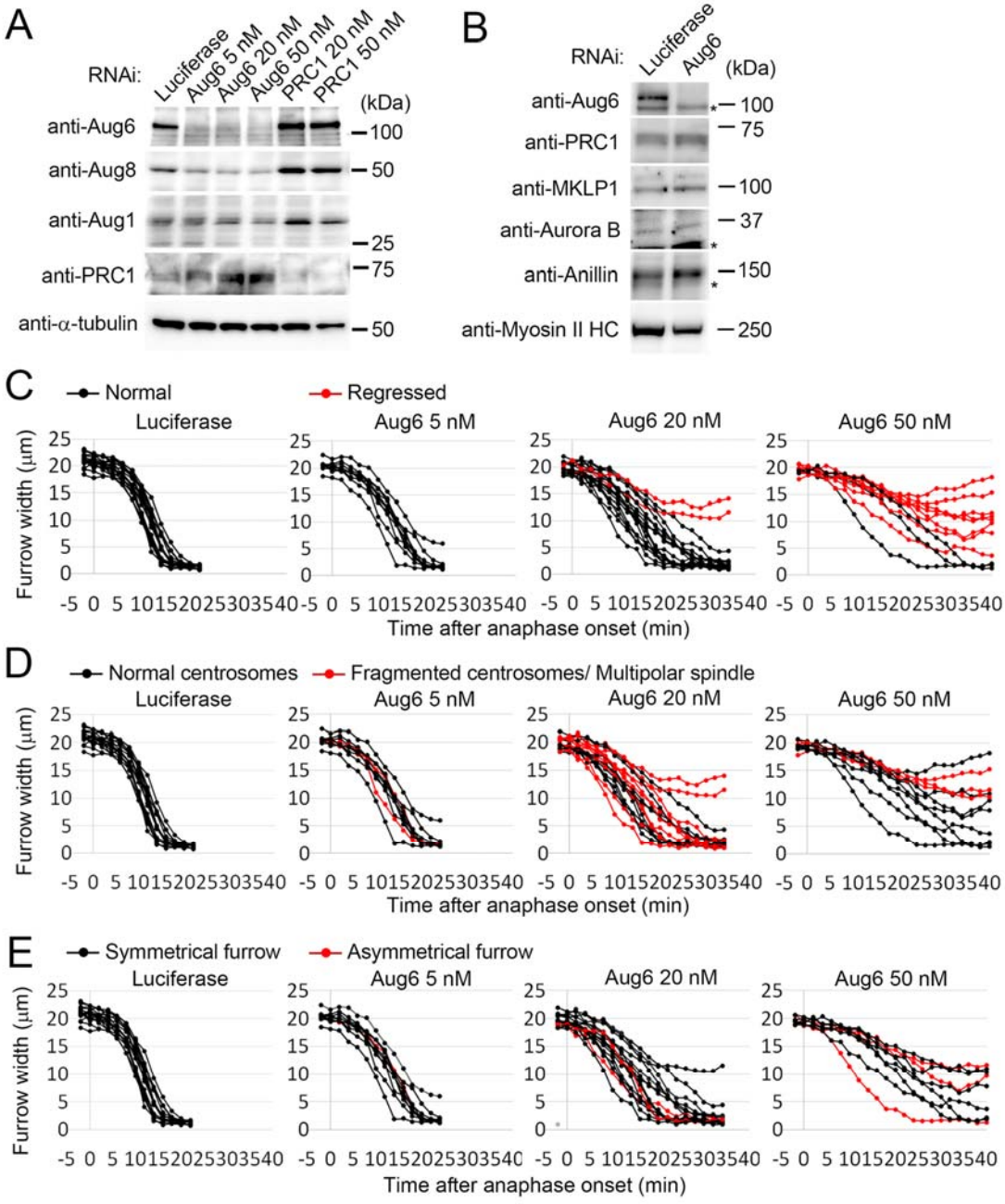
A
RNAi:
Luciferase
Aug6 5 nM
Aug6 20 nM
Aug6 50 nM
PRC1 20 nM
PRC1 50 nM
(kDa)
anti-Aug6
anti-Aug8
anti-Aug1
anti-PRC1
anti-α-tubulin
100
50
25
75
50
B
RNAi:
Luciferase
Aug6
(kDa)
anti-Aug6
anti-PRC1
anti-MKLP1
anti-Aurora B
anti-Anillin
anti-Myosin II HC
100
75
100
37
150
250
C
Normal
Regressed
Luciferase
Aug6 5 nM
Aug6 20 nM
Aug6 50 nM
Furrow width (μm)
Time after anaphase onset (min)
D
Normal centrosomes
Fragmented centrosomes/ Multipolar spindle
Luciferase
Aug6 5 nM
Aug6 20 nM
Aug6 50 nM
Furrow width (μm)
Time after anaphase onset (min)
E
Symmetrical furrow
Asymmetrical furrow
Luciferase
Aug6 5 nM
Aug6 20 nM
Aug6 50 nM
Furrow width (μm)
Time after anaphase onset (min)

Figure S1 (continued)

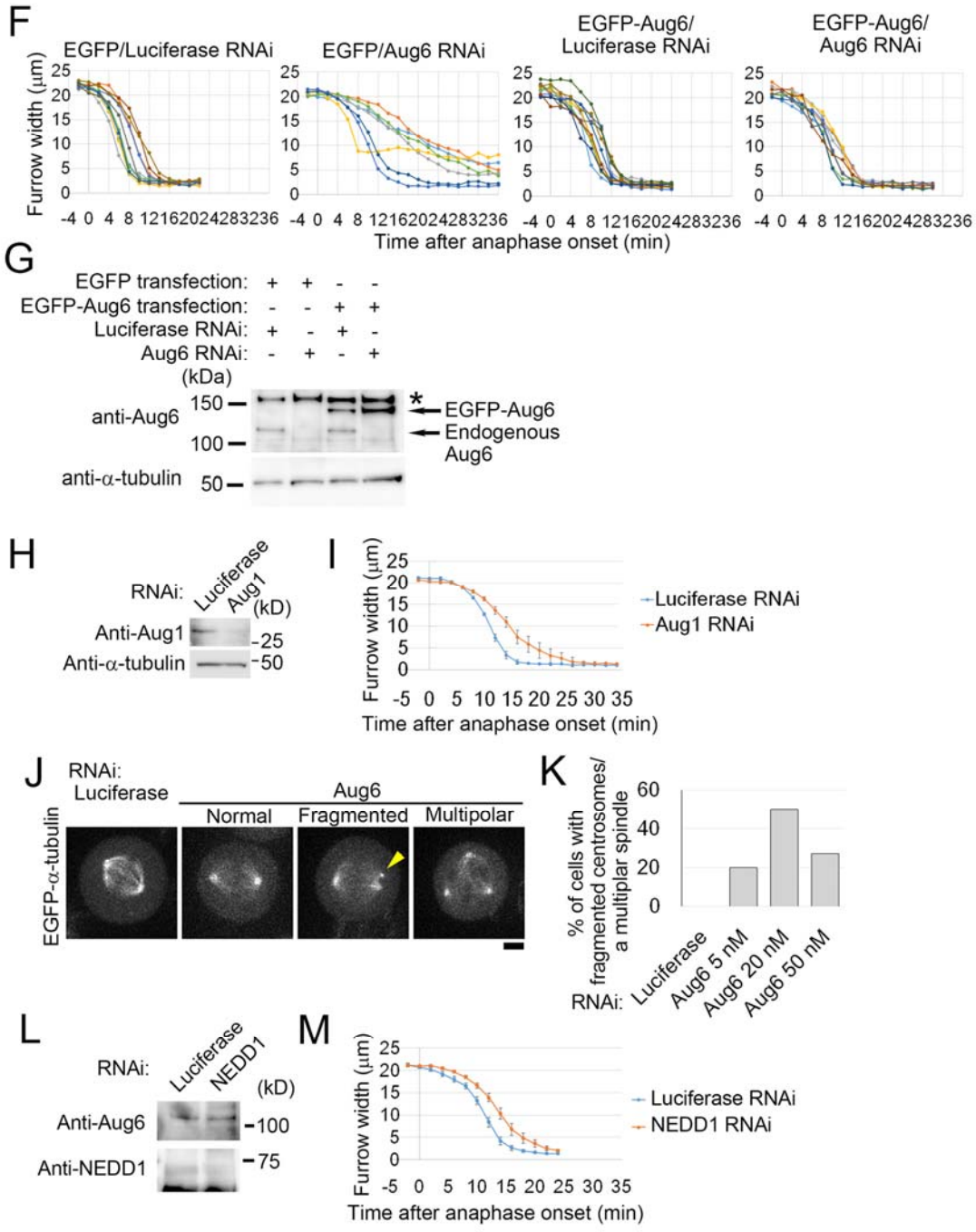

Figure S1: Cytokinesis defects caused by augmin or NEDD1depletion

(**A**, **B**) Immunoblotting against RNAi-treated HeLa cell extracts using antibodies against augmin subunits, PRC1 or α-tubulin(**A**), or against various cytokinesis regulators (**B**).Asterisk indicates non-specific signals. (**C**-**E**) Raw data for the time plot shown in

Figure 1**F**. Data points derived from cells that regressed during furrow ingression (**C**), that had fragmented centrosomes or a multipolar spindle (**D**), or that showed asymmetrical furrow ingression (**E**) are shown in red. Note that data points from cells that regressed too early to judge their symmetry were omitted in **E**.(**F**) Raw data for the time plot shown in Figure 1**H**. (**G**) Immunoblotting against the extracts from RNAi-treated HeLa cellsexpressing EGFP or an RNAi-resistant version of EGFP-Aug6 using antibodies against Aug6 or α-tubulin (as a loading control).Asterisk indicates non-specific signals.(**H, L**) Immunoblotting against RNAi-treated HeLa cell extracts using an anti-Aug1 antiserum (**H**), or anti-NEDD1 antibodies and anti-Aug6 antiserum (**L**). (**I, M**) Time plot of furrow width change in control and Aug1-depleted (**I**) or NEDD1-depleted (**M**) EGFP-α-tubulin cells. Mean ± SE of ≥7 cells from two independent experiments (**I**), or ≥11 cells from three independent experiments per condition(**M**).(**J**) Examples of spindle pole disorganization observed in Aug6-depleted EGFP-α-tubulin cells.The yellow arrowhead indicates a centrosome fragment.Scale bar, 5 μm.(**K**) Frequencies of spindle pole disorganization in RNAi-treated EGFP-α-tubulin cells. At least 10 cells from two independent experiments per condition were analyzed.

Figure S2

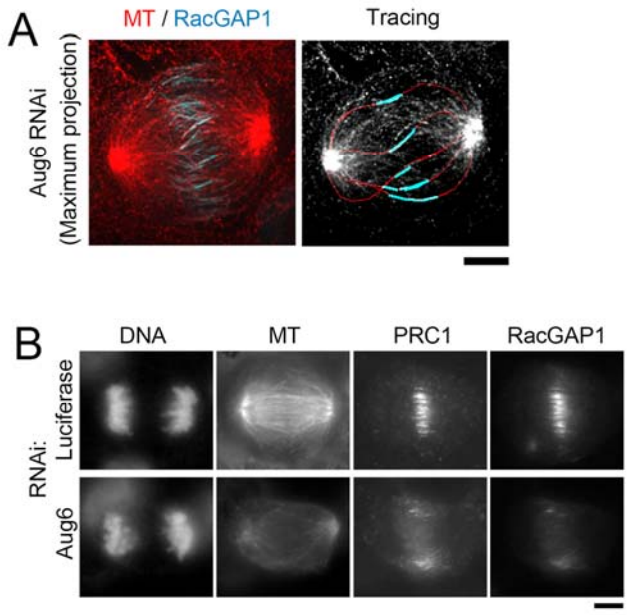

Figure S2: Astral MT bundles form in Aug6-depleted cells

(**A**) Left: Maximum projected images of immunostaining for RacGAP1 and MTs in an Aug6-depleted early anaphase cell. Right: tracing of MT antiparallel bundles (MT bundles in red, RacGAP1 positive regions in cyan). (**B**) Immunostaining of MTs, PRC1,

and RacGAP1, and staining of chromosomes by DAPI in control or Aug6-depleted cells.Scale bars, 5 μm.

Figure S3

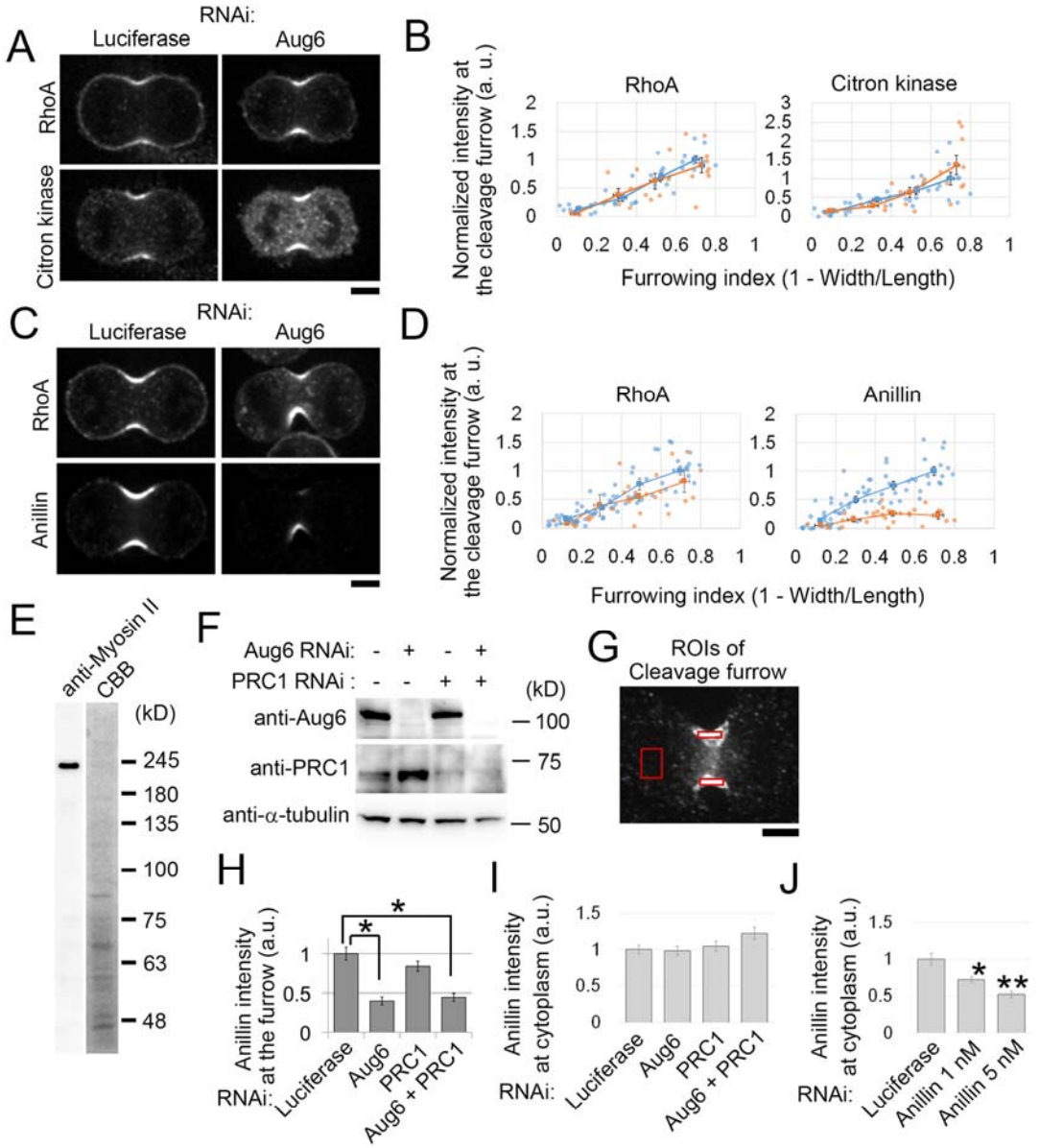

Figure S3 (continued)

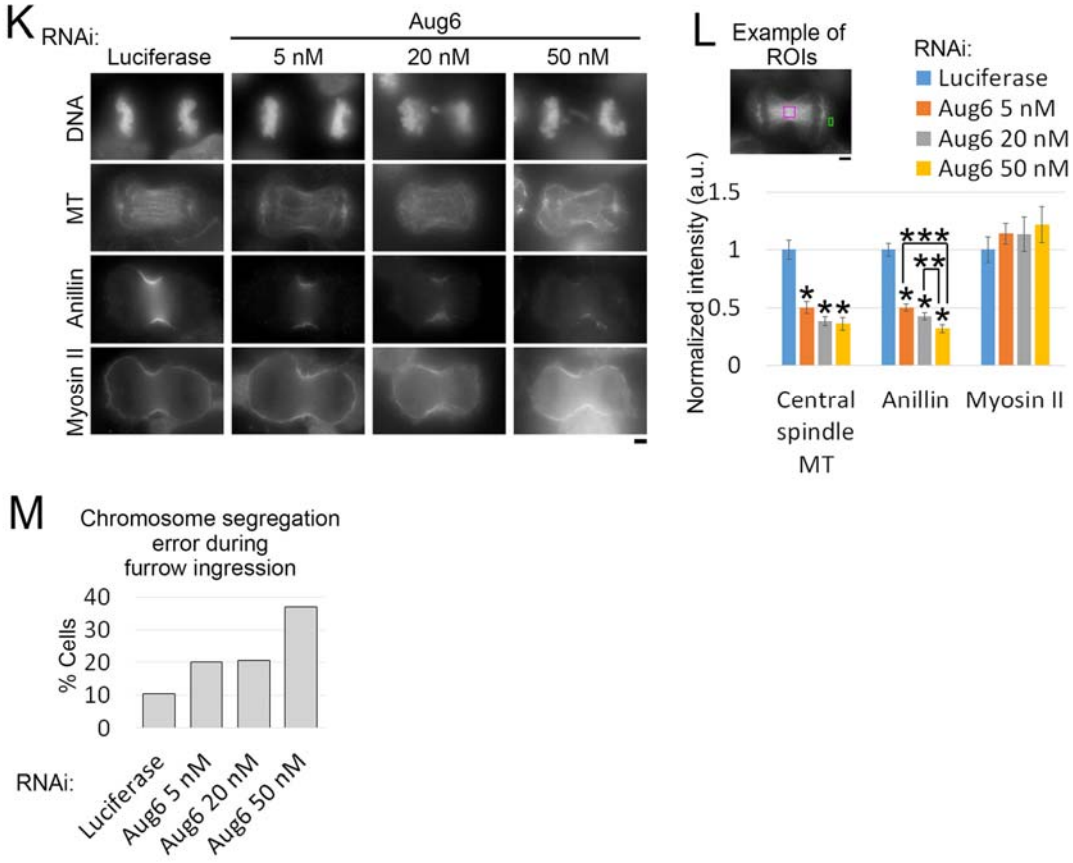

Figure S3: Specific mislocalization of anillin in Aug6-depleted cells

(**A**-**D**) Co-immunostaining of RhoA with citron kinase (**A**), or anillin (**C**) in control or Aug6-depleted cells. Quantification of signal intensity of RhoA and citron kinase (**B**), or anillin(**D**) at the cleavage furrow was carried out as described in Figure 3**F**.At least 22

cells (B), or ≥26 cells (D) from two independent experiments per condition were analyzed. (**E**) Immunoblotting against HeLa cell extracts using an anti-myosin IIA heavy chain antiserum. (**G**) Example of the ROIs used for quantification shown in Figures 4**B**, S3**H**-**J**, and S5**B**.(**H**) Normalized intensity of anillin staining at the cleavage furrow in RNAi-treated cells. Mean ± SE of ≥12 cells from two independent experiments per condition. Asterisks indicate statistically significant differences ($p < 0.001$, *t*-test).(**I, J**) Normalized intensity of anillin in the cytoplasm in RNAi-treated cells. Mean ± SE of ≥13 (**I**) or ≥10 cells (**J**) from two independent experiments per condition. The cytoplasmic level of anillin was significantly decreased following depletion of anillin (*, $p < 0.01$; **, $p < 10^{-5}$, *t*-test) (**J**), whereas it remained unchanged following depletion of either Aug6 or PRC1 (**I**). (**K**) Co-immunostaining of anillin, myosin IIA and α-tubulin in cells treated with various concentrations of Aug6 siRNA. (**L**) Normalized intensity of anillin and myosin IIA immunostaining at the cleavage furrow and that of α-tubulin at the cell center(central spindle MT) in the cells shown in K.For quantification of central spindle MT intensity, immunostaining signals of α-tubulin (magenta box) were subtracted bythe cytoplasmic background (green box) (top).Anillin and myosin IIA signals at the cleavage furrow were quantified as described in Figure 3E. Mean ± SE of ≥24 cells from two independent experiments per condition. Asterisks indicate statistically significant differences from control or between the indicated conditions(* $p < 10^{-5}$,** $p < 0.05$, *** $p<10^{-5}$,*t*-test). (**M**) Frequencies of chromosome segregation defects observed in the cells shown in K. At least 27 cells from two independent experiments per condition were analyzed.

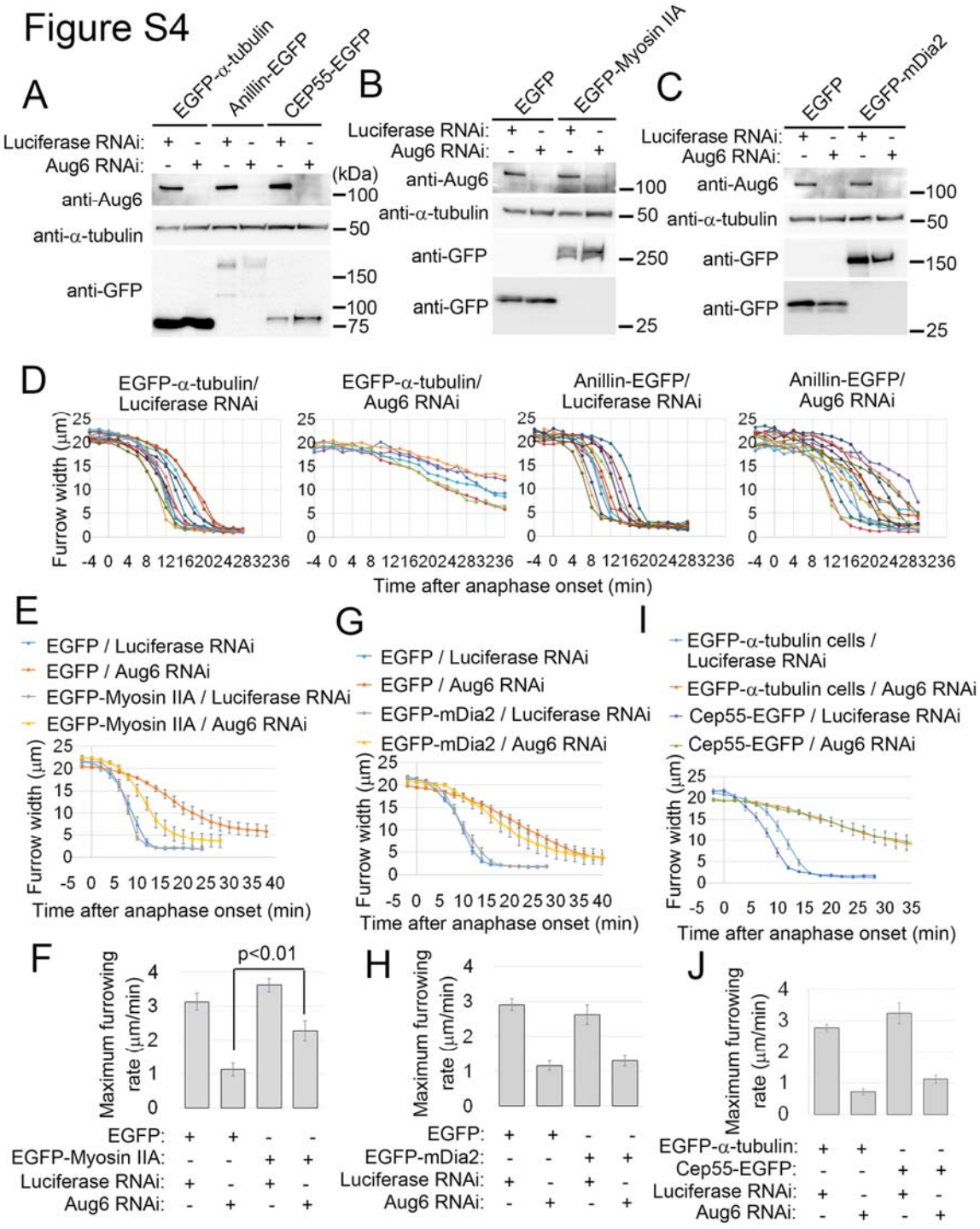

Figure S4: Effects of exogenous expression of various cell division regulators on the progression of cytokinesis in augmin-depleted cells

(**A-C**) Immunoblotting against extracts of RNAi-treated cells expressing EGFP-α-tubulin,anillin-EGFP, EGFP-Cep55 (**A**), or EGFP, EGFP-myosin IIA (**B**), or EGFP-

mDia2 (**C**)using antibodies against Aug6 or GFP. Endogenous α-tubulin protein was used as a loading control.(**D**) Raw data for the time plot shown in Figure 4**C**. (**E-J**) Time plot of furrow width change (**E**,**G**, **I**) and maximum furrowing rate (**F**, **H**, **J**) in RNAi-treated cells expressing EGFP or EGFP-myosin IIA (**E** and**F**), EGFP or EGFP-mDia2 (**G** and**H**), or EGFP-α-tubulin- or Cep55-EGFP (**I** and **J**). Mean ± SE of ≥6cells from two independent experiments (p value of the*t*-test) (**E** and **F**),≥7 cells from two independent experiments (**G** and **H**), or ≥7 cells from three independent experiments per condition (**I** and **J**).

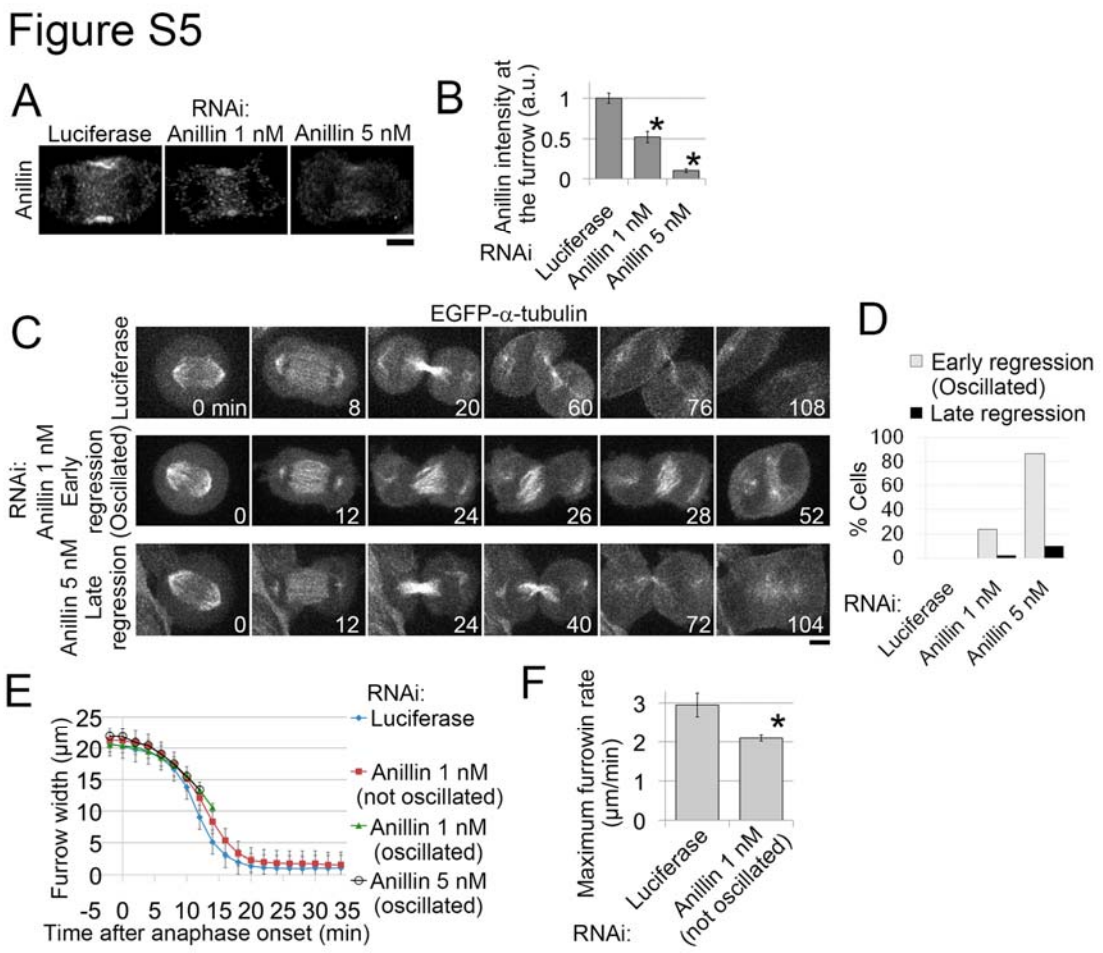

Figure S5: Cytokinesis defects in anillin-depleted cells

(**A**) Immunostaining for anillin in control and anillin-depleted cells. (**B**) Normalized intensity of anillin at the cleavage furrow. Mean ± SE of ≥10 cells from two independent experiments per condition. Asterisks indicate statistically significant differences from

control cells ($p < 0.001$, *t*-test). (**C**) Time lapse images of control or anillin-depleted EGFP-α-tubulin cells. Examples of cells that regressed during furrow ingression (early regression) or after furrow closure (late regression) are shown. Time after the onset of anaphase is indicated. (**D**) Frequencies of cytokinesis defects in control or anillin-depleted cells. At least 13 cells from three independent experiments per conditionwere analyzed. (**E, F**) Time plot of furrow width change (**E**) and maximum furrowing rate (**F**) in control and anillin-depleted EGFP-α-tubulin cells. Mean ± SE of ≥6 cells from two independent experiments per condition. Asterisk indicates a statistically significant difference ($p < 0.001$, *t*-test). Scale bars, 5 μm.

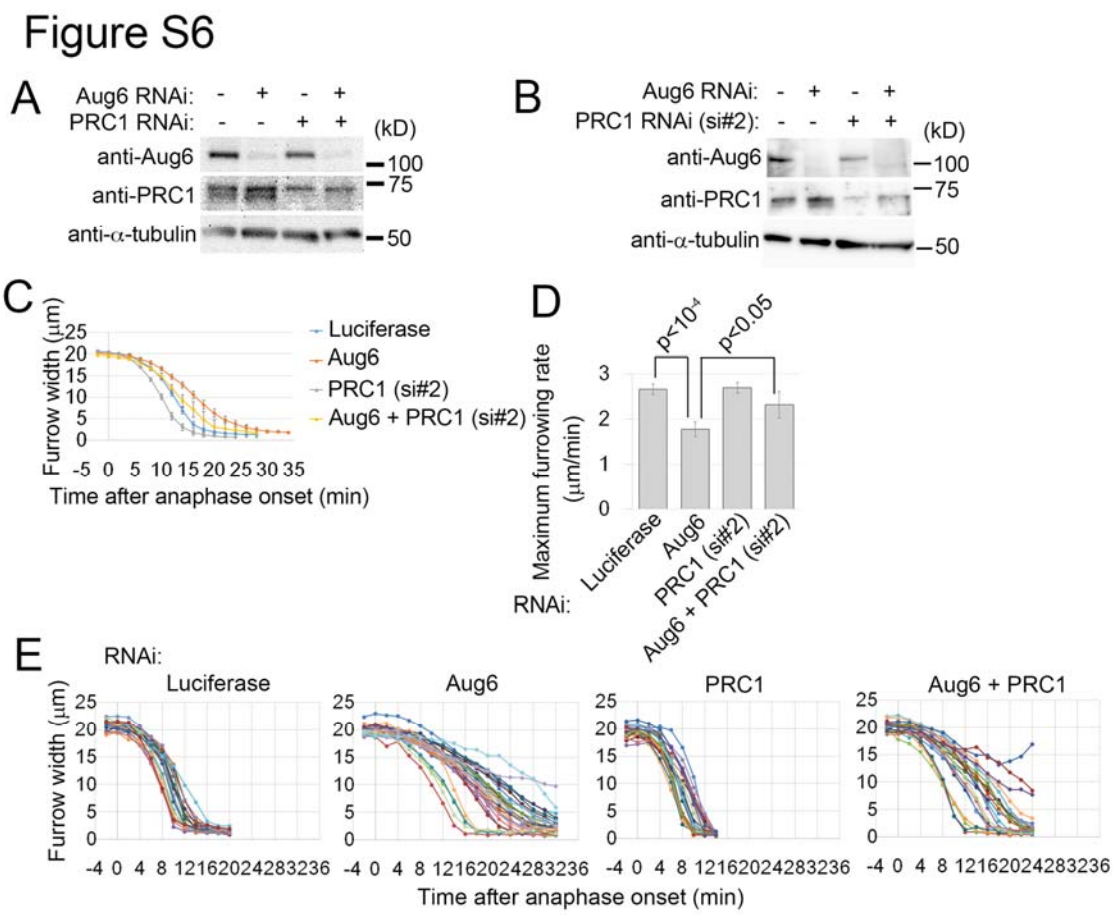

Figure S6: Formation of peripheral MT bundles in Aug6-depleted cells

(**A, B**) Immunoblotting against RNAi-treated HeLa cell extracts using anti-Aug6 or PRC1 antisera. PRC1 was depleted with siRNA#1 in **A**, and siRNA#2 in **B**. Endogenous α-tubulin was used as a loading control. (**C,D**) Time plot of furrow width change (**C**) and

maximum furrowing rate (**D**) in RNAi-treated EGFP-α-tubulin cells. Mean ± SE of ≥8 cells from three independent experiments per condition (p value of the *t*-test).(**E**) Raw data for the time plot shown in Figure 5**D**.

Figure S7

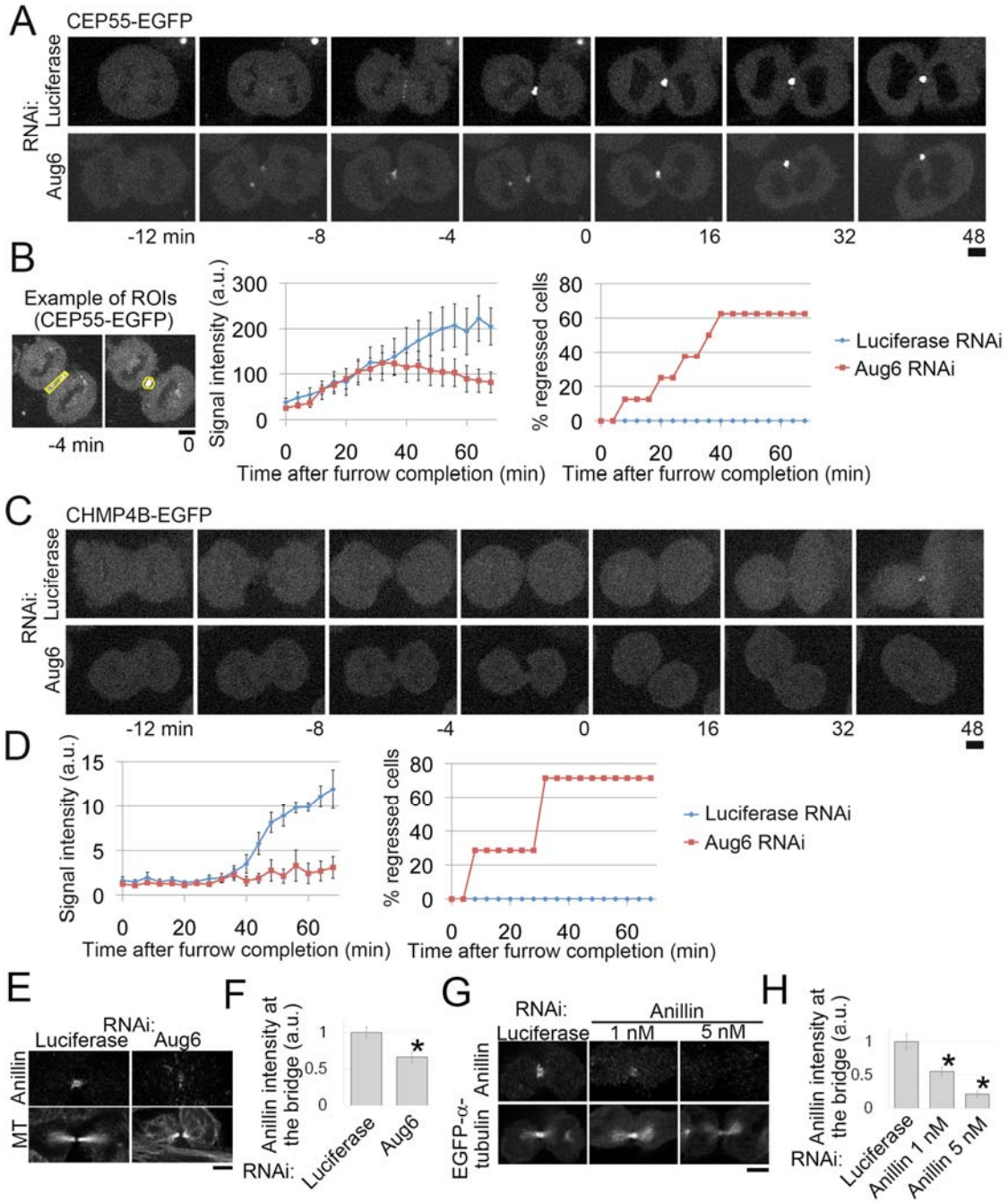

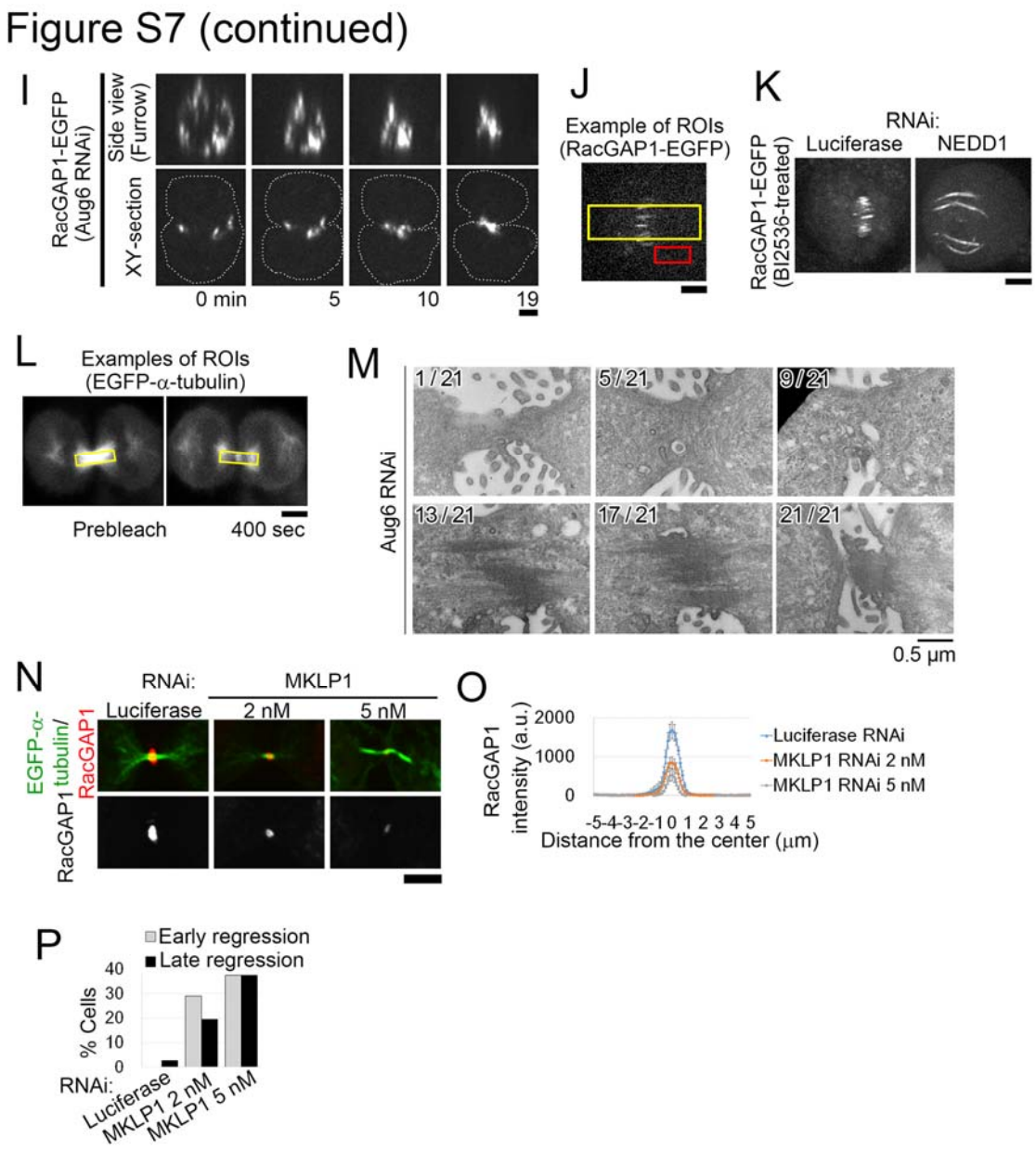

Figure S7: Late cytokinesis defects in Aug6-depleted cells

(**A**, **C**) Time-lapse images of RNAi-treated CEP55-EGFP (**A**) or CHMP4B-EGFP (**C**) cells. Time of furrowing completion was set at 0 min. (**B**, **D**) Time plot of GFP signal intensity (mean ± SE) at the intercellular bridge or a cumulative curve of regression

frequency after furrowing completion in RNAi-treated CEP55-EGFP or CHMP4B-EGFP cells (≥8 cells from four independent experiments in **B**, or ≥7 cells from two independent experiments per condition in **D**). Examples of ROIs used for the quantification are shown on the left in **B**. (**E, G**) Immunostaining for anillin and MTs (**E**) or EGFP-α-tubulin (**G**) in RNAi-treated cells. (**F, H**) Normalized intensity of anillin staining at the intercellular bridge in **E**(**F**) or **G** (**H**). Mean ± SE of ≥21 cells (**F**) or ≥7 cells (**H**) from two independent experiments per condition. Asterisks indicate statistically significant differences ($p < 0.01$ in **F**, and $p < 0.001$ in **H**, *t*-test). (**I**) ZX-plane projection (at the cleavage furrow area) and XY-plane confocal section of a RacGAP1-EGFP cell depleted of Aug6. (**J, L**) Examples of ROIs used in the quantification shown in Figure 7F (**J**) or 7H(**L**). (**K**) Control and NEDD1-depleted RacGAP1-EGFP cells treated with MG132 and BI2536 for 40 min before fixation. (**M**) Serially sectioned TEM images of the intercellular bridge in an augmin-depleted cell.Numbers indicate each section (per total sections: each section was 75 nm thick). (**N**) Immunostaining for RacGAP1 in control or MKLP1-depleted EGFP-α-tubulin cells. (**O**) Line profiles of RacGAP1 immunostaining intensity along the division axes in control and MKLP1-depleted EGFP-α-tubulin cells. Mean ± SE of ≥10 cells from two independent experiments per condition. (**P**) Frequencies of cytokinesis defects in control or MKLP1-depleted cells. At least 31 cells from two independent experiments per conditionwere analyzed.Scale bars, 5 μm, except for **M**.